

# Holographic Interferometry Real Time Imaging of Refraction Index 2D Distribution and Surface Deformations in Biomedicine

N. A. Davidenko<sup>1</sup>, X. Zheng<sup>2</sup>, I. I. Davidenko<sup>1</sup>, V. A. Pavlov<sup>1</sup>, N. G. Chuprina<sup>1</sup>, N. Kuranda<sup>1</sup>, S. L. Studzinsky<sup>1</sup>, A. Pandya<sup>2</sup>, H. Mahdi<sup>2</sup>, A. Ladak<sup>2</sup>, C. Gergely<sup>3</sup>, F. Cuisinier<sup>3</sup> and A. Douplik<sup>2,4</sup>

<sup>1</sup>Taras Shevchenko National University, 64/13, Volodymyrska Street, City of Kyiv, 01601, Ukraine

<sup>2</sup>Photonics Group, Department of Physics, Ryerson University, 350 Victoria Street, Toronto, M5B 2K3, Canada

<sup>3</sup>Université de Montpellier, 34090, Montpellier, France

<sup>4</sup>Keenan Research Centre of the LKS Knowledge Institute, St. Michael Hospital, Toronto, M5B 1W8, Canada

**Keywords:** Holography, Interferometry, Imaging, Holography Interferometry, Double Exposure Holography, Holography Interferometry Imaging, Photodynamic Therapy, Dentistry, Biomedicine.

**Abstract:** Holographic Interferometry of 2D Imaging of Refraction Index and Surface Deformations were recorded in real time video: (1) monitoring of local refraction index perturbation at accuracy of  $10^{-4}$  in transmission mode during heat and photochemical reactions with human hemoglobin using methylene blue, protoporphyrin IX and rhodamine as the photosensitizers and (2) monitoring in reflectance mode of human tooth local mechanical pressure at accuracy of  $10^{-7}$ m.

## 1 INTRODUCTION

In this study, we explored potentials of holography interference imaging in transmission and reflectance modes. The transmission mode was exploited to map the refraction index modifications inside the phantom while the reflectance mode was employed to monitor the surface displacement map of the human tooth.

We explored photochemical and photothermal reaction due to interaction of light and hemoglobin at presence of a photosensitizer. Hemoglobin was selected as a component of blood that is the main absorber of light in visible range. Blood is the main oxygen supplier of biotissues and oxygen is one of the key components of photodynamic therapy (PDT). Blood is also a main carrier of photosensitizers (PSs) administrated systemically – orally or intravenously. PDT is a non-surgical treatment modality based on photochemical reactions and administrated as a part of clinical routine in Europe, Japan, Australia, North and South America (Wilson B.C., Patterson, M.S., 2008). PDT is an extremely precise and controllable light-based therapy targeting malignant lesions, mostly focusing on those that develop across significant areas (e.g., esophageal cancer) or relatively shallow depth (GI tract, prostate), or applied as an antimicrobial therapy (Hamblin MR,

Hasan T., 2004). Within the biophotonics market sector, PDT demonstrates the highest growth, almost 40% annually (Biophotonics Market, Tematys, 2013). Pharmaceutical companies, such as Axcan, Parmaceuticals Inc, Nigma, Glaxo-Wellcome Inc, DUSA, Photocure, Galdderma and others have become important players in PDT.

The physical processes involved in the PDT interaction of laser beam and material are divided into three parts: (1) absorption of the light energy; (2) transformation of this energy into chemical energy and/or into heat; (3) ultimate chemical reaction and/or phase transformation. In some cases, it is difficult to distinct hyperthermal and photochemical reactions, hence in the study at the current stage we consider the both effects taking place.

PDT is a photochemical reaction involving (1) light, (2) photosensitive molecules (photosensitizer) absorbing light and (3) ambient molecular oxygen ( $O_2$ ) generating reactive oxygen species (ROS), which in turn destroy biotissue cells or extracellular matrix (Dougherty, T.J. et al, 1998). These include the Type I (sensitizer-substrate) and Type II (sensitizer-oxygen) reactions. Type II photochemical reactions (Fig. 1) represent the transfer of light energy to the molecular oxygen conversion into singlet oxygen ( $^1O_2$ ). In this study, we presume only the

second type of oxygen dependent photochemical reaction which comes with release of  $^1\text{O}_2$  taking into account the photosensitizer used in the study – Methylene Blue. Methylene Blue is an FDA-approved clinical dye, which also can be used as a photosensitizer (Foster TH et al., 2010). The II type of PDT reaction leads to both depletion of dissolved molecular oxygen and eventually to conversion of oxygenated to reduced form of hemoglobin (Douplik A., Stratonnikov A., Loschenov V et al., 2011), and to photobleaching or photodegradation of the photosensitizers. An example of such conversions from the previous studies is demonstrated in Fig. 2 a,b. The transformation of hemoglobin from the oxygenated to deoxygenated form is clearly observed, confirming oxygen consumption during PDT (Fig. 2a). The photosensitizer photobleaching during PDT without a substantial change in the spectral line shape is demonstrated in Fig. 2b. Absorption and fluorescence spectroscopy and imaging have been successfully applied in reflectance mode for PDT monitoring (Dougherty et al., 1998). However, currently there are no monitoring techniques that can be applied for PDT in optically transparent tissues and organs such as eye. This study is an attempt to develop a PDT monitoring technology capable to register reactions in optically transparent tissues based on local alterations of the refractive index, exploiting the model reaction with human hemoglobin, which was previously successfully studied and described by absorption and fluorescence methods.

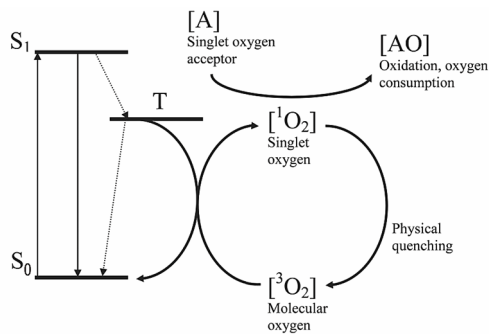


Figure 1: Jablonski diagram of the processes during second type of PDT reaction (via singlet oxygen generation mechanism) (Modified from Douplik A., Stratonnikov A., Loschenov V et al, 2011).

Holographic interferometry monitoring of hyperthermal and photochemical reactions with human hemoglobin have been conducted under control of the sample absorption spectra.

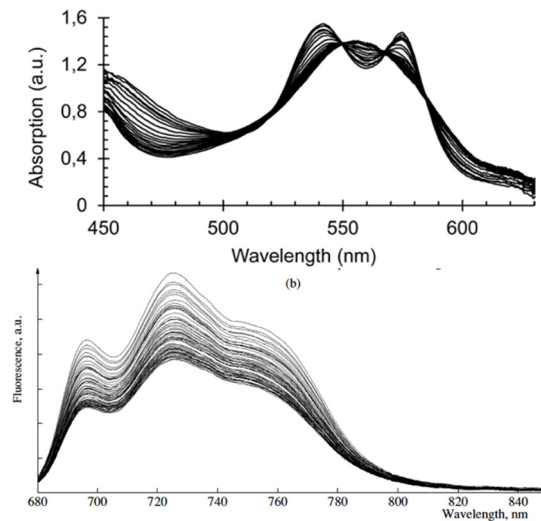


Figure 2: a) The absorption spectra variation in blood sample incubated with Methylene Blue during laser irradiation. The initial two-hump spectrum of oxygenated hemoglobin ( $\text{HbO}_2$ ) transformed into a single peak spectrum of reduced hemoglobin (RHb) as a result of PDT reaction. b) Fluorescence spectra from a blood sample incubated with Phtalocyanine Aluminum (Photosence) as the photosensitizer at a concentration of  $20 \mu\text{M}$ . Laser fluence rate is  $25 \text{ mW/cm}^2$  at  $670 \text{ nm}$ . The time interval between spectra is  $20 \text{ s}$ . (Modified from Douplik A., Stratonnikov A., Loschenov V et al, 2003, 2011).

In dentistry, there is a demand to assess how the tooth undergoes by mechanical pressure in case of counter implants. Identification of particular points of high mechanical pressure and pressure gradients is required.

## 2 MATERIALS AND METHODS

### 2.1 Materials

Lyophilised human hemoglobin powder (H7379 Sigma-Aldrich, USA) was used for this study component, replacing red blood cells, as it is readily available and easily handled. Due to the process of lyophilisation approximately 80-85% of the hemoglobin is methemoglobin (MetHb). Sodium dithionite (S310-100 Fisher Scientific) was added to MetHb in phosphate buffered solution (PBS) (Multicell sterile, Wisent inc., Canada) to form reduced haemoglobin (HbR) which was then oxygenated to form oxyhaemoglobin ( $\text{HbO}_2$ ) according to the procedure described in our previous paper (Zhernovaya, Sidoruk, Tuchin, Douplik, 2011) providing ultimate concentration  $0.5 \text{ g/L}$ .

Photosensitizers Protoporphyrin IX (PPIX, Sigma-Aldrich, USA) and Rhodamine (Sigma-Aldrich, USA) were added to the solution creating concentrations of 0.05g/L and 0.02 g/L accordingly. Half of the samples with PPIX were created in liquid form, and the other half was prepared on 300-Bloom gelatin derived from acid-cured porcine skin (G2500, Sigma-Aldrich Corp., St. Louis, MO) forming polymerized samples. The samples with Rhodamine were created only in liquid form. The control samples included: (1) PBS, (2) PBS/10%-gelatin, (3) PBS/0.5g/L Hb, (4) PBS/0.05g/L PPIX, (5) PBS/10%-gelatin/0.5 g/L Hb, (6) PBS/10%-gelatin/0.05g/L PPIX, (7) - PBS/0.02g/L Rhodamine. 3 samples were used in each experimental group including both the control and PPIX experiments. For Rhodamine control and experiment were used 2 samples per group.

## 2.2 Experimental Setup

The absorption spectra were measured on Shimadzu UV-3600 spectrophotometer (Japan). The Holography Interference setup is depicted in Fig. 3 and described in (Derzhypolska L., Davidenko N., 2006).

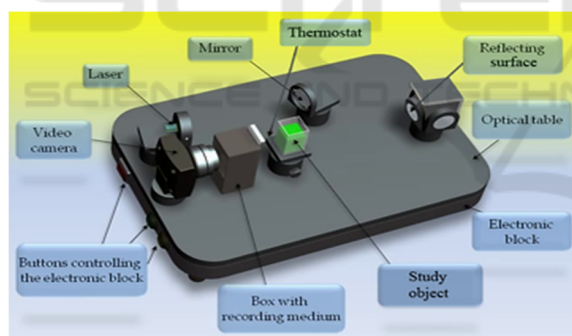


Figure 3: Double exposure real time Holography Interferometry setup.

A black-and-white web camera was used for experiment with PPIX and for the Rhodamine experiment we used a RGB camera (Basler ac-A2000-165uc, Basler AG, Germany). Red laser diode was employed for holography (660 nm, 4mW, INTEGRAF LLC, USA) and green laser diode (532 nm, 50 mW, Thorlabs, USA) used for irradiation providing the irradiance of 62 mW/cm<sup>2</sup>. A long pass interference filter (Comar Optics, UK) was exploited to facilitate both the irradiation of the sample and holography interference imaging acquisition.

The monitoring of PDT reactions was carried out in transmission mode, while monitoring of the surface displacement map of the human tooth was conducted in reflectance mode.

## 2.3 Data Processing

Fringe images was processed with carrier frequencies. Fringe patterns with carrier frequencies are processed using the Fourier transform method discussed earlier in introduction. A Matlab function that includes an automatic and a manual implementation of the method was obtained from Matlab File Exchange (mathworks.com/fileexchange/53421). The user of the GUI is given the option of manually selecting the side peak in the Fourier spectrum representing  $c(x,y)$ , or an automatic option can be used but the user has to specify the width of the side peak in the Fourier spectrum. Increasing the width avoids negating phase information but allows for more noise to be included.



Figure 4: (a) noisy fringe pattern; (b) noisy extracted phase using the Fourier transform method; (c) denoised phase using WFT.

In addition, the user is given an option to use a windowed Fourier transform after demodulation in order to denoise the obtained phase before unwrapping at the cost of significantly increasing processing time. The application of a windowed Fourier transform (WFT) for fringe analysis was first proposed in (Qian Kemao, 2004). The combination of the Fourier transform method and the WFT was tested and proven to be successful. Figure 4 shows the effectiveness of using the WFT method in denoising phase.

## 3 RESULTS AND CONCLUSIONS

The holography interference images for control experiments are depicted in Fig. 5 (a snapshot from the video clip at 60th second). A partial formation of the first interference ring can be observed only in case of PBS/10%-gelatin/0.5 g/L Hb sample (Fig. 5 c), which apparently was caused by the hyperthermal effect, while the control samples with PBS/gelatin

and Methylene Blue/gelatin (Fig. 5a, b) did not manifest any registerable photochemical reaction.

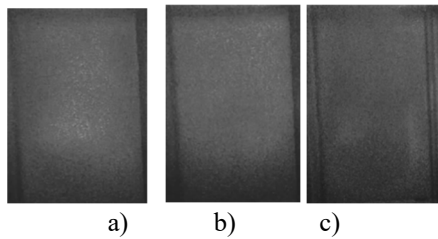


Figure 5: Holography interference images for control experiment (60<sup>th</sup> second snapshot): a) gelatin only; b) gelatin plus Methylene Blue; c) gelatin plus Hemoglobin. The contours of the cuvette walls are clearly seen.

The holography interference images for Methylene Blue experiment are shown in Fig. 6 demonstrating a significant reaction forming ca. 5 interference rings, which approximately matches a modification of the refraction index by 5 folds.

Preliminary we could conclude that contributions of photochemical reactions are considerably higher than a pure heating effect. Once the green laser irradiation was switched off, in the experimental samples the refraction index returned back to its original values within 60 seconds.

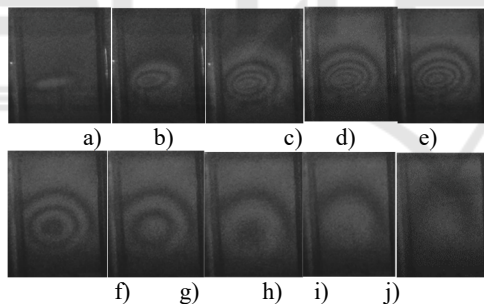


Figure 6: Holography interference snapshot from video clip images for Methylene Blue experiment arranged in seconds of irradiation: a) 2 s; b) 10 s, c) 30 s, d) 59 s, e) 60s (laser is switched off), f) 65 s (5 seconds later after laser switched off), g) 70 s, h) 80 s, i) 90 s, k) 120 s. The long pass filter was set in front of the camera to let a minor leak of the irradiation green light to expose onto the side walls of the cuvette for monitoring the irradiation condition consistency (a-d). The laser was switched off in the frames e-j. The white circle in the center of the interference pattern of the first frame (a) is the irradiation spot location (not scaled, the diameter of the spot was 1.5 mm).

As a result of the work, the heat and photochemically induced reactions with human hemoglobin have been successfully monitored by holography interference method towards development of PDT monitoring technology in transparent tissues.

The holography interference images for PPIX experiment are depicted in Fig. 7. A formation of the interference ring can be observed. The holography interference images for Rhodamine C experiment are depicted in Fig. 8. The control samples with PBS, gelatin and PPIX did not manifest any photochemical reaction. The control samples with HbO<sub>2</sub> only have shown some reactions but much less than that of with PPIX plus HbO<sub>2</sub> experiments even after 60 seconds of irradiation.

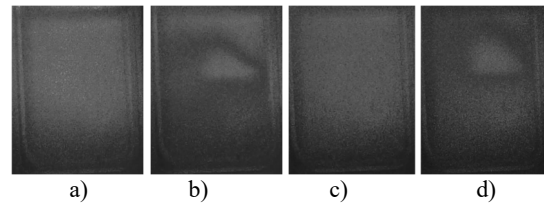


Figure 7: Holography interference images for PPIX experiment: a) liquid sample before irradiation; b) liquid sample, beginning of the reaction (25th second); c) gelatin sample before laser irradiation; d) gelatin sample, beginning of the reaction (12th second).

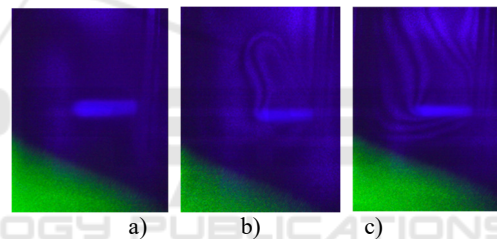


Figure 8: Holography interference images for Rhodamine C experiment: a) liquid sample before irradiation; b) liquid sample, beginning of the reaction (2nd second), c) liquid sample, development of the reaction (4th second). The long pass filter was set in front of the camera to let a minor leak of the irradiation green light to expose onto the bottom left corner of the frame for monitoring the irradiation condition consistency. The light rod shape in the center of the frame is the irradiation spot.

The reaction without photosensitizer was interpreted as a pure heating effect. Once the green laser irradiation was off, in the gelatin samples the RHb have been completely oxygenated back during 1-2 minutes. Such a fast resurrection of RHb to HbO<sub>2</sub> has not been observed in liquid samples.

Holography interference images in reflectance mode for tooth before and after applying mechanical pressure are shown in Fig. 9 a,b. The mechanical pressure was applied from the top. Estimated displacement of the surface was ca. 80 nm.

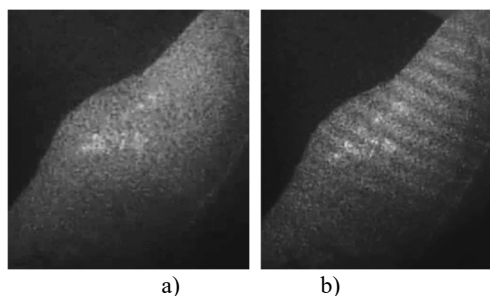


Figure 9: Holography interference images for tooth before applying mechanical pressure (a) and after (b). The mechanical pressure was applied from the top. Estimated displacement of the surface was ca. 80 nm.

The heat, photochemically induced reactions with human hemoglobin and surface deformation due to mechanical pressure have been successfully monitored by holography interference method towards development of monitoring technology in both transparent and opaque tissues for biomedicine.

## ACKNOWLEDGEMENTS

This study was supported by the Natural Sciences and Engineering Research Council of Canada (NSERC), Personal Discovery Grant (Douplik A), Ryerson University Health Research Grant. Aman Ladak was supported by NSERC Engage grant.

## REFERENCES

- Wilson B.C., Patterson, M.S. The physics, biophysics and technology of photodynamic therapy. *Phys. Med. Biol.*, 53, R61–R109, (2008).
- Hamblin MR, Hasan T. Photodynamic therapy: A new antimicrobial approach to infectious diseases? *Photochem Photobiol Sci.* 4;3: 436–50, (2004)
- Biophotonics Market Technologies and Market Analysis, Tematys, Cortesy of EPIC, (2013).
- Dougherty, T. J., Gomer, C.J., Henderson, B.W., Jori, G., Kessel, D., Korbek, M., Moan, J., Peng, Q. Photodynamic therapy. *J. Nutl. Cancer Znst.*, 90, 889-905, (1998).
- Baran T. M., Giesselman B. R., Hu R, Biel MA, Foster TH."Factors influencing tumor response to photodynamic therapy sensitized by intratumor administration of methylene blue." *Lasers in surgery & medicine*, 42(8):728-35 (2010)
- Douplik A., Stratonnikov A., Zhernovaya O. and Loschenov V. "Modifications of Blood Optical Properties during Photodynamic Reactions in Vitro and in Vivo", Chapter 20 in "Advanced optical cytometry:

- methods and disease diagnoses", Edited by V.V. Tuchin, Wiley-VCH, (2011)
- Stratonnikov A., Douplik A., Loschenov V., "Oxygen Consumption and Photobleaching in Whole Blood Incubated with Photosensitizer Induced by Laser Irradiation," *Laser Physics* 13 (1), 1-21, (2003)
- Zhernovaya O., Sidoruk O., Tuchin V., Douplik A., "The refractive index of human hemoglobin in the visible range", *Phys Med Biol.* 56(13): 4013-21 (2011)
- Derzhypolska L., Davidenko N., Medved N. and Pryadko L. "Holographic projection interferometer with photorefractive recording media", *Proc. SPIE* 6023, Tenth *International Conf. on Nonlinear Optics of Liquid and Photorefractive Crystals*, 60230O (December 06, 2006); doi:10.1117/12.648209 (2006)
- Matlab function for extraction of phase from interferogram. Retrieved August 16, 2017, from <https://www.mathworks.com/matlabcentral/fileexchange/53421-matlab-function-for-extraction-of-phase-from-interferogram>
- Kemao, Q., Windowed fourier transform for fringe pattern analysis. *Applied Optics*, 43(13), 2695-2702. (2004).